# Deciphering the Heat Sources Behind Time-Variant Subglacial Geothermal Areas in Iceland

Hannah I. Reynolds[1]*, Magnús T. Guðmundsson[1], Thórdís Högnadóttir[1] and Guðni Axelsson[2]

[1]Nordvulk, Institute of Earth Sciences, University of Iceland, Sturlugata 7, Reykjavík 101, Iceland

[2]Iceland GeoSurvey (ÍSOR), Grensásvegur 9, IS-108 Reykjavík, Iceland

*hir@hi.is

## ABSTRACT

Thermal anomalies at the Earth's surface are observed at volcanoes all over the world but are usually difficult to quantify. However, where thermal signals occur beneath glaciers, ice cauldrons (depressions on the ice surface) form due to melting at the glacier base; the ice acts as a calorimeter which allows for heat flux estimates to be made with considerable accuracy. This study explores the heat sources behind time-variant subglacial geothermal activity. The gradual collapse of the subglacial Bárdarbunga caldera in 2014–2015 lead to major changes in the geothermal activity around the caldera rim. Several weeks after the start of the collapse, significant growth occurred in three cauldrons on the caldera rims, with four smaller cauldrons forming in 2015–2017. Five years after the Bárdarbunga event, some cauldrons continue to grow whereas others do not. The cauldrons have reached volumes between $1.0\pm0.2$ and $27\pm3$ million m$^3$. Similarities are found between the activity at Bárdarbunga and rapid changes in geothermal activity at Grímsvötn, also associated with volcanic eruptions. In contrast, much longer-term geothermal activity has also been observed at Grímsvötn, and at Skaftárkatlar, where two cauldrons have been active for more than 80 years. HYDROTHERM numerical modelling software was used to simulate heat and mass transport in geothermal systems to investigate possible scenarios to explain the variations in geothermal activity observed at different time-scales. Shallow intrusions connected to high-permeability pathways were found to greatly enhance surface thermal signals. Pre-intrusion temperature of the surrounding bedrock has a major effect on heat transfer to the surface, where temperature conditions close to the boiling point of water produce efficient heat transfer due to the formation of steam plumes. This work improves the understanding of both rapid and years-to-decades scale variations in geothermal power.

## 1. INTRODUCTION

Thermal anomalies are observed at many locations in Iceland, resulting from geothermal and magmatic activity, and are usually difficult to quantify since the measurement of heat fluxes from the ground to the atmosphere is subject to large uncertainties. However, where these thermal signals occur beneath glaciers, a special situation is exploited, where the overlying ice acts as a calorimeter (e.g. Sigvaldason, 1965; Björnsson, 1983; Gudmundsson et al., 2004; Jarosch and Gudmundsson, 2007; Reynolds et al., 2017). This allows for estimates to be made of heat release, based on the volume of ice melted over a specified time period, and provides the opportunity to calculate the surface heat flux to a much improved accuracy, as all of the thermal energy is spent melting ice (Jarosch and Gudmundsson, 2007; Jarosch et al., 2008). Sub-glacial geothermal fields manifest as ice cauldrons (depressions in the glacier surface), which have been observed at several volcanoes in Iceland, e.g. Mýrdalsjökull, Eyjafjallajökull, Bárdarbunga, Grímsvötn, and Skaftárkatlar.

Thermal signals are also observed at many ice covered volcanoes worldwide (Major and Newhall, 1989). Notable examples outside Iceland include the ice caves observed at Mount St. Helens and Mount Rainier in the U.S.A. (Kiver and Mumma, 1971; Anderson et al., 1998; Zimbelman et al., 2000), and at Mount Erebus in Antarctica (Giggenbach, 1976). Several thermal features evolved at Redoubt volcano, Alaska, in the build-up to the 2009 eruption, including ice surface depressions, wide-spread subsidence, and punctures created by steam (Bleick et al., 2013).

Monitoring geothermal activity at volcanoes gives necessary insight into the associated volcanic and phreatic hazards, and the hydrothermal systems below. Fumaroles, hot springs, and bubbling mud pools characterise the surface expression of many geothermal areas (e.g. Hochstein and Bromley, 2001; 2005). This work improves our understanding of short- and long-term variations in hydrothermal systems, and how they may relate to magma movements and bedrock properties. Rapid ice melting at geothermal areas often results in jökulhlaups, which pose a threat to infrastructure and affected communities, and therefore the study of ice-covered geothermal fields is of use for hazard assessment (Gudmundsson et al., 2008; Edwards et al., 2015).

In this paper we explore the possible heat sources of the geothermal signals observed after three eruptions at Grímsvötn (1998, 2004 and 2011) and the eruption of Holuhraun in 2014-2015, where the magma originated from underneath the Bárdarbunga central volcano, causing a gradual caldera collapse (Sigmundsson et al., 2015; Gudmundsson et al., 2016). Further, we compare the energy released by geothermal activity at these two volcanoes, following recent eruptions, with the thermal energy released by the eruptions.

## 2. REGIONAL SETTING

### 2.1 Grímsvötn

Grímsvötn lies beneath the centre of Vatnajökull (figure 1), near the northern end of the Grímsvötn volcanic system, the most volcanically active system in Iceland in historic times (Larsen et al., 1998; Thordarson and Larsen 2007). Most of the eruptions originate from the caldera at Grímsvötn, which has produced six eruptions in the past 100 years (e.g. Björnsson and Gudmundsson, 1993; Oddsson et al., 2012; Jude-Eton et al., 2012; Hreinsdóttir et al., 2014). Grímsvötn comprises three caldera structures, with a partially subglacial lake located in the main caldera (Björnsson and Einarsson, 1990; Gudmundsson and Milsom, 1997). Meltwater

from the Grímsvötn area collects in the lake, and is released periodically as a jökulhlaup. Grímsvötn is one of the most geothermally active calderas in the world, with sustained heat output for centuries in the Gigawatts range (Björnsson, 1988). The geothermal activity is easily visible, with ice cauldrons forming around the caldera rims and steaming areas in the exposed bedrock and around the edges of the open parts of the lake. Geothermal activity at Grímsvötn has been the subject of many studies. Sigvaldason (1965) published the first estimates of the heat output at Grímsvötn, followed by studies by Björnsson in 1974 and 1988, and a detailed record of the heat output between 1922 and 1991 was published by Björnsson and Gudmundsson (1993). Annual changes in heat release in the eighteen years between 1998 and 2016, a period during which three eruptions took place within the Grímsvötn caldera, were reported by Reynolds et al (2018).
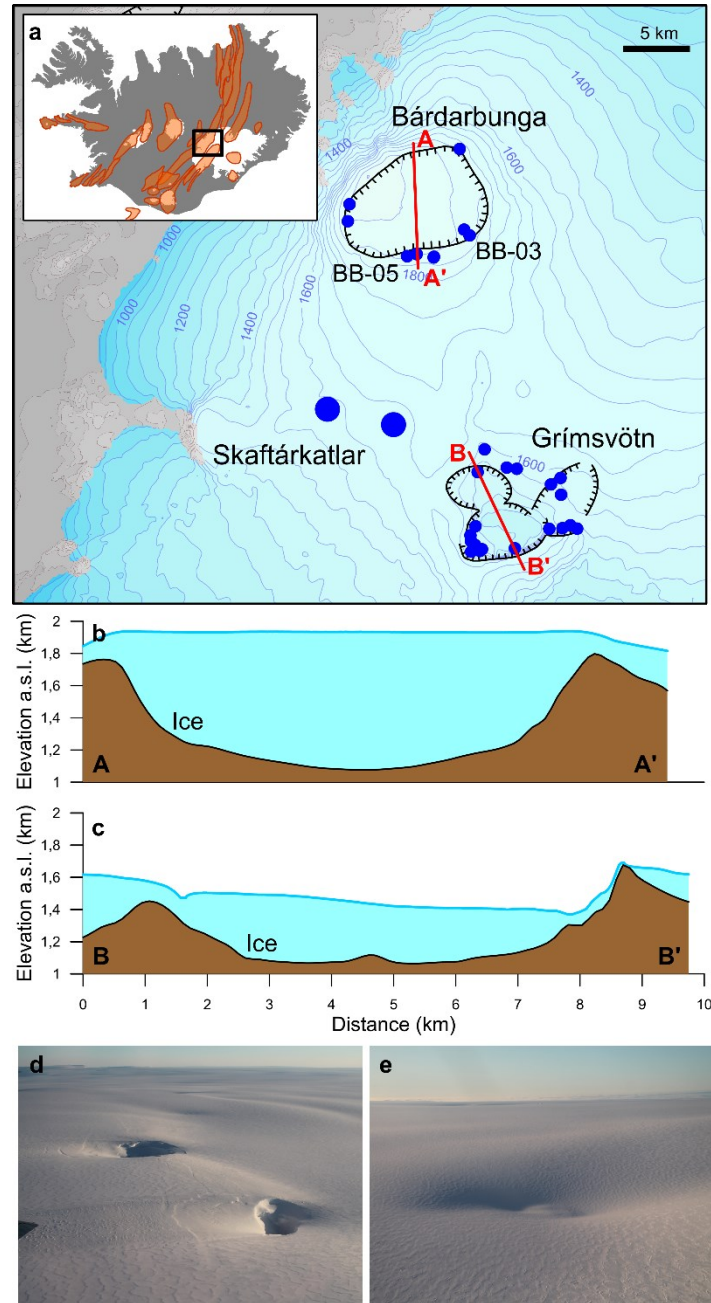


**Figure 1: Ice cauldrons in Vatnajökull. a) Map of the north-western part of Vatnajökull, with ice cauldrons displayed as blue circles. b) and c) are cross-sections through the Bárdarbunga and Grímsvötn calderas respectively. Cross-section paths shown on a). Bedrock surface from Björnsson and Einarsson (1990). d) and e) are photographs of ice cauldrons on the southern and western rims of Bárdarbunga respectively, taken in November 2018. The cauldrons in d) are 100-150 m wide while the depression in e) has a diameter of 700-800 m.**

### 2.2 Bárðarbunga

Bárdarbunga is a subglacial central volcano located in the north-west of Vatnajökull (figure 1). It is part of the Bárdarbunga-Veidivötn volcanic system, which has produced more than 20 known eruptions in the last 1200 years (Larsen et al., 1998; Óladóttir et al., 2011). It has a large caldera approximately 65 $km^2$ in area, with an ice thickness of 700–800 m at its deepest point (Björnsson and Einarsson, 1990). The most recent Bárdarbunga eruption took place in 2014–2015, in the form of a large fissure eruption which lasted for 6 months and produced ~1.5 $km^3$ of lava at the Holuhraun eruption site (Sigmundsson et al., 2015; Pedersen et al., 2017; Gudmundsson

et al., 2016). The 2014–15 Bárdarbunga-Holuhraun eruption was preceded by increased seismic activity within the Bárdarbunga caldera starting 16 August 2014. Ice subsidence was observed within the Bárdarbunga caldera during the eruption, with no evidence of significant basal melting, representing a slow caldera collapse (Gudmundsson et al., 2016). The heat output of preexisting minor subglacial geothermal areas at the caldera rim increased following the onset of seismic activity, and new cauldrons formed in the years following. These cauldrons were active for a minimum of 6 months, and some remain active. Ice cauldrons had been observed on the Bárdarbunga caldera rims prior to the 2014–15 event, both at the western and south-eastern parts of the caldera rim. The western cauldron has been sustained for decades and is geothermally generated (Eiríksdóttir, 2012).

The south-eastern cauldrons were formed after the Gjálp eruption in 1996 (Gudmundsson et al., 2004). These may have formed due to minor subglacial eruptive activity (Kristmannsdóttir et al., 1999). In the 18 years between the Gjálp eruption in 1996 and the onset of activity in Holuhraun in 2014, geothermal activity in this location was intermittent, with a shallow cauldron being visible in some years and not in others.

## 3. METHODS

Ice cauldrons are shallow depressions which form on the glacier surface due to basal melting, as a manifestation of heat flux from below (e.g. Björnsson 1976; Jarosch and Gudmundsson, 2007); the melting ice acts as a calorimeter, allowing estimations of heat flux magnitude to be made. The heat source may either be a subglacial eruption or geothermal activity. Several types of thermal signals are observed, with the onset time, duration, and location of the resulting cauldrons all being important factors. Geothermally generated cauldrons tend to produce a sustained signal over months, years, or decades. The ice surface at Grímsvötn is mapped annually, in June, using primarily GPS data (Reynolds et al., 2018). The Bárdarbunga ice cauldrons are mapped using airborne radar altimetry profiling (Reynolds et al., 2019), and satellite imagery. The ice surface elevation maps are used to calculate ice cauldron volumes, which can be used to estimate the thermal energy ($Q$) required to produce the observed cauldrons using:

$$Q = (U + 1)\rho_i V_i L_i + \rho_i A b L_i$$

where $U$ is an underestimation factor of 23% (Jarosch and Gudmundsson, 2007), used to correct for the inflow of ice into the cauldrons which leads to an underestimation of the ice melted if only visible volume change is included; $\rho_i$ is the ice density, for which a value of 917 kg m$^{-3}$ is used; $V_i$ is the volume of the depression (ice cauldron); and $L_i$ is the latent heat of fusion for ice, for which $3.34 \times 10^5$ J kg$^{-1}$ is used. The second term accounts for the surface accumulation of ice, where $A$ is the area around the ice cauldron from which ice is expected to flow into the cauldron, b is the surface accumulation per year (water equivalent), and is ~2 m/year for Bárdarbunga and averaged ~1.35 m/year for Grímsvötn during the study period (Björnsson and Pálsson, 2008; Pálsson et al., 2016). The ice is assumed to be at melting point at the base of the glacier, and therefore no heat is required to increase the ice temperature to its melting point. Possible heat stored as in a water body beneath the glacier at temperatures above 0°C is not considered either, but it can be shown that such heat is minor compared with the overall thermal energy required to meltthe ice.

The energy per unit time released at the glacier base by geothermal activity is referred to in this paper as geothermal power. Following a volcanic eruption, the total energy released is found by integrating over time the contributions from individual cauldrons.

For volcanic eruptions, the maximum heat output of eruptive products is given by:

$$E_e = M_e \left[ L + C \left( T_i - T_f \right) \right]$$

Here $M_e$ is the total erupted mass, $C$ is the temperature-averaged specific heat capacity of the material erupted, $T_i$ is magmatic temperature (assumed to be 1130°C) and $T_f$ the ambient temperature where the erupted material is deposited. The value used here is $T_f = 0$°C. For the 2014-15 eruption of Holuhraun-Bárdarbunga, the erupted material is lava and the latent heat of crystallization is also released, taken as $L = 4 \times 10^5$ J kg$^{-1}$ for basalt (Sphera et al., 2000). For the eruptions in Grímsvötn considered here, the erupted products are tephra, and therefore no crystallization occurs, and $L$ is assumed to be zero.

## 4 THERMAL SIGNALS

### 4.1 Bárðarbunga

BB-03 is located in an area of known previous geothermal activity and began to grow within a month of the onset of increased seismic activity at Bárdarbunga in August 2014 (figure 1). It continued to grow for a period of years following the eruption, with sporadic geothermal activity. Cauldrons were observed on the southern caldera rim in July 2015 (including BB-05; figure 1), five months after the end of the eruption. The maximum geothermal power is 700-800 MW, observed in 2014 during the eruption, with a second peak in 2017.
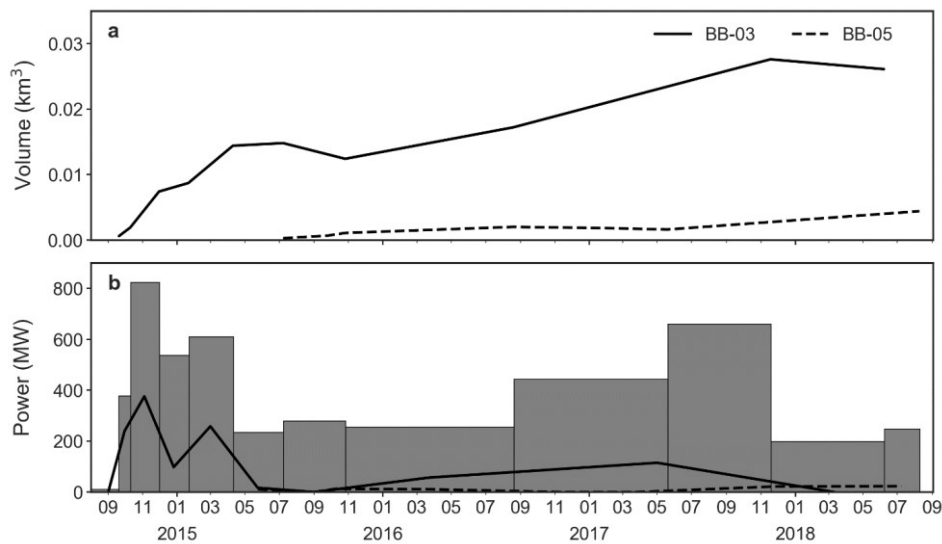
**Figure 2: Formation and growth of the Bárdarbunga ice cauldrons since 2014. a) Volumes of Bárdarbunga cauldrons BB-03 and BB-05. b) Bars give the combined geothermal power of the Bárdarbunga cauldrons, with the solid and dashed lines showing the geothermal power at BB-03 and BB-05 respectively. Modified after Reynolds et al., 2019.**

### 4.2 Grímsvötn

The geothermal signal following eruptions at Grímsvötn in 1998, 2004, and 2011 are displayed in figure 3 (see Reynolds et al. 2018 for details on the data). For the 1998 and 2011 eruptions an increase in geothermal power is observed during the eruption year and the following year, before it decreases. However, in the years following the 2004 eruption, a steady increase in geothermal power is observed.
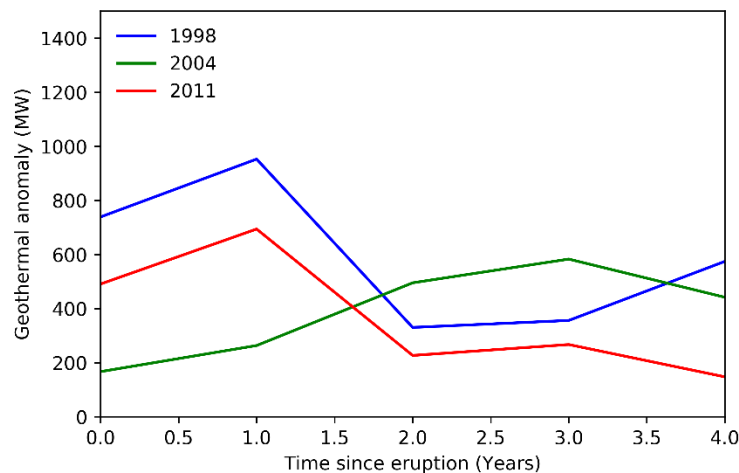


**Figure 3: Changes to geothermal power at Grímsvötn following the eruptions of 1998, 2004 and 2011.**

### 4.3 Relationship between eruption size and geothermal activity

The maximum heat output of the erupted material is compared with the observed geothermal anomaly following the eruption (figure 4). The mass erupted in each eruption is after Reynolds et al. (2018) and references therein. The values used are:

G1998:  8 x $10^7$ m³ of tephra, or 1.0 x $10^{11}$ kg, using tephra density of 1190 kg m⁻³ for Grímsvötn tephra (Oddsson et al., 2012).

G2004:  5.6 x $10^{10}$ kg (Oddsson et al., 2012)

G0211:  ~7 x $10^8$ m³ of tephra, or ~8 x $10^{11}$ kg.

Bárdarbunga-Holuhraun 2014-2015:  1.44 x $10^9$ m³ of lava (Pedersen et al., 2017), ~3.7 x $10^{12}$ kg, using lava density 2600 kg m⁻³.

The graph in figure 4 shows that, although the energy from erupted magma varies over two orders of magnitude, the range in geothermal energy released varies only by a factor of 5. The Grímsvötn eruptions of 1998 and 2004 have associated geothermal anomalies of around half of the heat emitted by erupted products, 55% and 44% respectively, assuming the upper value of geothermal anomaly. Whereas the much larger Grímsvötn eruption of 2011 has an associated anomaly of 5% that of the heat emitted. The Bárdarbunga-Holuhraun eruption produced a geothermal signal far smaller relative to the heat emitted by erupted products, of just 0.3%.
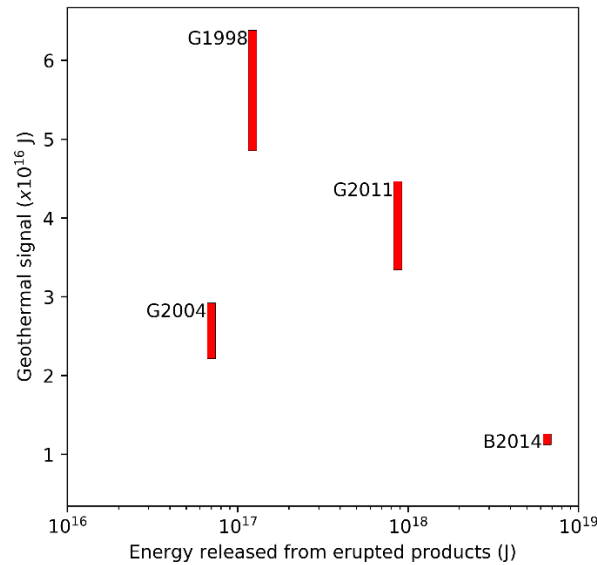
**Figure 4: Geothermal energy released in the first three years following an eruption compared with the total heat emitted by erupted material (tephra for the Grímsvötn eruptions of 1998, 2004 and 2011, lava in the case of Holuhraun-Bárdarbunga 2014). It is not trivial to isolate the geothermal signals associated with the eruptions, so this value is given as a range, denoted by rectangles.**

## 6. DISCUSSION

The relationship between the heat released by erupted material and the associated geothermal anomalies varies significantly for the smaller Grímsvötn eruptions (1998 and 2004), the Grímsvötn 2011 eruption, and the 2014–2015 Bárdarbunga-Holuhraun eruption. The smaller Grímsvötn eruptions have a much higher associated geothermal anomaly relative to the eruption size. This may indicate that the volume of shallow intrusions, that are suspected to be the main heat source for the anomalies in geothermal power observed, varies much less than the volume of erupted material. In terms of change in activity, the events in Bárdarbunga are much more drastic than in Grímsvötn. Grímsvötn is a very active geothermal area, even during periods of eruptive quiescence. In contrast, only weak geothermal activity had been observed at Bárdarbunga prior to the 2014–2015 event (Eiríksdóttir, 2012; Reynolds et al., 2019). Thus, Bárdarbunga activity over the first years after the caldera collapse resembles that of Grímsvötn. However, it remains to be seen how long-lived the presently observed geothermal output of Bárdarbunga will be.

Reynolds et al., 2019, use HYDROTHERM to gain insight into the surface thermal signals generated by shallow magmatic intrusions. HYDROTHERM is a numerical modelling program available from the U.S.G.S., which simulates multi-phase ground-water flow and thermal energy transport at termperatures of up to 1200 °C (Hayba and Ingebritsen, 1997; Kipp et al., 2008). They simulate heat flow from a shallow magmatic intrusion to the surrounding bedrock, focusing on the surface heat flux. Shallow intrusions into high permeability pathways were found to generate a rapid surface signal. The pre-intrusion temperature of the surrounding bedrock has a major effect on heat transfer to the surface, with cold bedrock causing a buffering effect, whereas temperature conditions close to the boiling point of water produce far more efficient heat transfer due to the formation of steam plumes (figure 5).
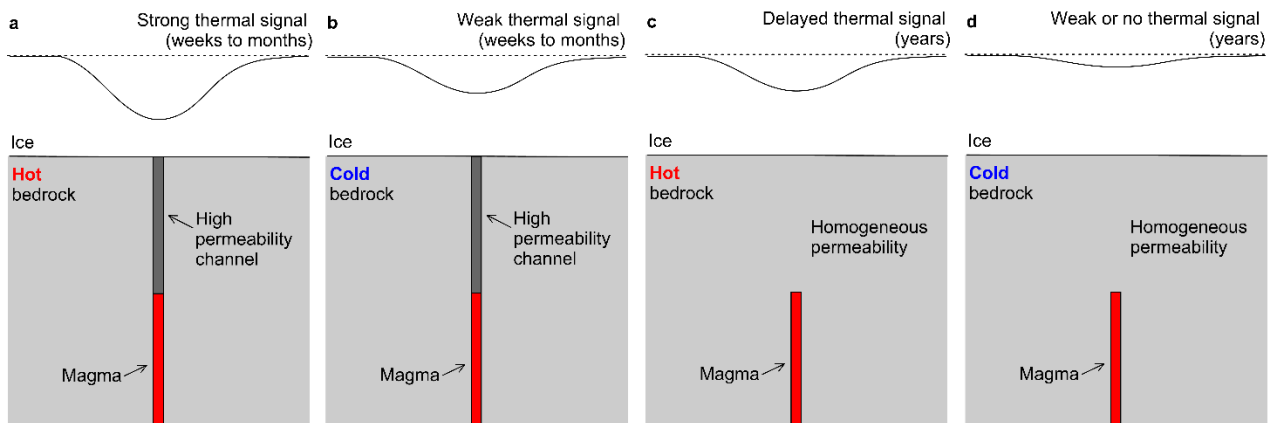


**Figure 5: Schematic diagrams of cauldron formation under different conditions, based on results from Reynolds et al. (2019). a) Hot bedrock with intrusion meeting high permeability channel. b) Cold bedrock with intrusion meeting high permeability channel. c) Hot bedrock with magma intruded into rock with homogeneous permeability. d) Cold bedrock with magma intruded into rock with homogenous permeability. The type of signal and the onset time from intrusion to cauldrons formation is noted at the top of the diagrams.**

Reynolds et al.

The geothermal anomalies that established very quickly after the start of eruptions (e.g. BB-01, BB-02, BB-03, and some of the cauldrons at Grímsvötn; Reynolds et al., 2018;2019) may be the product of shallow intrusions into high permeability pathways. Other signals which appear to be related to eruptive activity, but with a delay, may be due also to increased permeability, but a less direct pathway to the surface. The sporadic geothermal signals observed at some cauldrons, e.g. BB-03, may be due to 'steam plumes' which can form in hydrothermal systems around intrusions (Reynolds et al., 2019).

In contrast to the months-to-years long geothermal signals observed at Bárðarbunga following the Holuhraun eruption, and at Grímsvötn following recent eruptions, longer term geothermal signals (decades) are also observed at Grímsvötn (Björnsson, 1988: Björnsson and Gudmundsson, 1993). Another example of long-term activity is Skaftárkatlar, two geothermally generated ice cauldrons, located in the western part of Vatnajökull ice cap outside the boundaries of known central volcanoes (figure 1). They are presently amongst the most powerful geothermal areas in Iceland with their combined power exceeding 1 GW, having grown by an order of magnitude in the last 80 years (Gudmundsson et al., 2018). No volcanic eruptions were observed over this period although their growth may have been related to increased seismicity observed after 1950 in this part of Vatnajökull (Brandsdóttir, 1984).

## 7. CONCLUSIONS

We present time series of thermal signals from Bárðarbunga following the 2014-2015 eruption, and for Grímsvötn following the 1998, 2004, and 2011 eruptions. The main conclusions are:

- An increase in geothermal power is observed during the eruption year and the following year for the 1998 and 2011 Grímsvötn eruptions, before it decreases. In the years following the 2004 eruption, a steady increase in geothermal power is observed.
- The Grímsvötn eruptions of 1998 and 2004 were followed by geothermal signals of approximately 50% of the value of heat emitted by erupted material, and the Grímsvötn 2011 and Bárðarbunga-Holuhraun 2014 eruptions resulted in respective geothermal signals of 5% and 0.3% of the heat emitted by erupted material.
- Rapidly formed ice cauldrons are observed at both Bárðarbunga and Grímsvötn, associated with volcanic eruptions. It is likely that these formed due to shallow intrusions.

## REFERENCES

Anderson CH, Behrens CJ, Floyd GA, Vining MR (1998) Crater Firn Caves of Mount St. Helens, Washington. *J Caves and Karst Stud* 60:44–50.

Björnsson, H. (1976). Marginal and supraglacial lakes in Iceland. *Jökull,* 26, 40

Björnsson, H. (1983). A natural calorimeter at Grímsvötn. *Jökull*, 33, 13-18.

Björnsson, H. (1988). Hydrological characteristics of the drainage system beneath a surging glacier. *Nature*, 395(6704), 771.

Björnsson, H., Einarsson, P. (1990). Volcanoes beneath Vatnajökull, Iceland: evidence from radio-echo sounding, earthquakes and jökulhlaups. *Jökull* 40:147–148.

Björnsson, H., Guðmundsson, M.T. (1993). Variations in the thermal output of the subglacial Grímsvötn caldera, Iceland. *Geophys. Res. Lett.* 20, 2127–2130.

Björnsson, H., & Pálsson, F. (2008). Icelandic glaciers. *Jökull*, 58(58), 365-386.

Bleick, H.A., Coombs, M.L., Cervelli, P.F., Bull, K.F.,Wessels, R.L., 2013. Volcano-ice interactions precursory to the 2009 eruption of redoubt volcano, Alaska. J. Volcanol. Geotherm. Res. 259, 373–388.

Brandsdóttir, B., (1984). Seismic activity in Vatnajökull 1900-1982 with special reference to Skeiðarárhlaups, Skaftárhlaups and Vatnajökull eruptions. *Jökull*, 34, 141-150.

Edwards, B.R., Gudmundsson, M.T., and Russell, J.K. (2015). Glaciovolcanism. In Sigurðsson H, Houghton B, McNutt S, Rymer H, Stix J, editors, Encyclopedia of Volcanoes, pp. 377– 393. Elsevier, Boston.

Eiríksdóttir VS (2012) Þróun sigkatla í Bárðarbungu (Bachelor´s thesis). Retrieved from http://skemman.is/stream/get/1946/11961/30211/1/BS.pdf.

Giggenbach, W.F. (1976). Geothermal ice caves on Mt Erebus, Ross Island, Antarctica. New Zeal *J Geol Geophys* 19:365–372, doi:10.1080/00288306.1976.10423566.

Gudmundsson, M.T., and Milsom, J. (1997). Gravity and magnetic studies of the subglacial Grímsvötn volcano, Iceland. Implications for crustal and thermal structure. *J Geophys Res* 102: 7691–7704.

Gudmundsson, M.T., Sigmundsson, F., Björnsson, H., and Högnadóttir, Th. (2004). The 1996 eruption at Gjálp, Vatnajökull ice cap, Iceland: efficiency of heat transfer, ice deformation and subglacial water pressure. *Bull. Volcanol*. 66 (1), 46–65.

Gudmundsson, M.T., Högnadóttir, Þ., Kristinsson, A.D. and Guðbjörnsson, S. (2007). Geothermal activity in the subglacial Katla caldera, Iceland, 1999–2005, studied with radar altimetry. *Annals of Glaciology* 45: 66-72.

Gudmundsson, M.T., Larsen, G., Höskuldsson, Á., and Gylfason, Á.G. (2008). Volcanic hazards in Iceland. *Jökull* 58:251–268.

Gudmundsson, M.T., Jónsdóttir, K., Hooper, A. et al (2016). Gradual caldera collapse at Bárðarbunga volcano, Iceland, regulated by lateral magma outflow. *Science* 353:aaf8988. doi:10.1126/science.aaf8988

Gudmundsson, M.T., Magnússon, E., Högnadóttir, Þ., Pálsson, F. and Rossi, C. (2018). Hættumat vegna jökulhlaupa í Skaftá. Skaftárkatlar – saga og þróun 1938-2018. (Hazard assessment due to jökulhlaups in river Skaftá, Skaftárkatlar, evolution history 1938-2018). Veðurstofa Íslands og Jarðvísindastofnun Háskólans, VÍ 2018-17, RH-16-2018. 62 pp.

Hayba, D.O., and Ingebritsen, S.E. (1997). Multiphase groundwater flow near cooling plutons. *J Geophys Res* 102(B6): 12,235-12,252.

Hochstein, M.P., and Bromley, C.J. (2001). Steam cloud characteristics and heat output of fumaroles. *Geothermics* 30:547–559.

Hochstein, M.P., and Bromley, C.J. (2005). Measurement of heat flux from steaming ground. *Geothermics* 34:133–160.

Hreinsdóttir, S., Sigmundsson, F., Roberts, M.J., Björnsson, H., Grapenthin, R., Arason, P., Árnadóttir, T., Hólmjárn, J., Geirsson, H., Bennett, R.A., Gudmundsson, M.T., Oddsson, B., Ófeigsson, B.G., Villemin, T., Jónsson, T., Sturkell, E., Höskuldsson, Á., Larsen, G., Thordarson, T., and Óladóttir, B.A. (2014). Volcanic plume height correlated with magma pressure change at Grímsvötn Volcano, Iceland. *Nature Geoscience* 7:214–218, doi:10.1038/ngeo2044

Jarosch, A.H., Gudmundsson, M.T. (2007). Numerical studies of ice flow over subglacial geothermal heat sources at Grímsvötn, Iceland, using full stokes equations. *J. Geophys. Res*. 112, F02008. https://doi.org/10.1029/2006JF000540.

Jarosch, A.H., Gudmundsson, M.T., Högnadóttir, T., and Axelsson, G., (2008). Progressive cooling of the hyaloclastite ridge at Gjálp, Iceland, 1996–2005. *J. Volcanol. Geotherm. Res*. 170, 218–229.

Jude-Eton, T.C., Thordarson, T., Gudmundsson, M.T., and Oddsson, B. (2012). Dynamics, stratigraphy and proximal dispersal of supraglacial tephra during the ice-confined 2004 eruption at Grímsvötn Volcano, Iceland. *Bull Volcanol* 74(5):1057–1082.

Kipp, K.L., Hsieh, P.A., and Charlton, S.R. (2008). Guide to the revised ground-water flow and heat transport simulator: HYDROTHERM — Version 3: U.S. Geological Survey Techniques and Methods 6–A25, 160 p.

Kiver, E., and Mumma, M. (1971). Summit firn caves, Mount Rainier, Washington. *Science* 173:320–322.

Kristmannsdóttir H, Björnsson A, Pálsson, S, Sveinbjörnsdóttir ÁE (1999) The Impact of the 1996 Subglacial Volcanic Eruption in Vatnajökull on the River Jökulsá Á Fjöllum, North Iceland. J Volcanol Geotherm Res 92(3–4): 359–72. doi:10.1016/S0377-0273(99)00056-6.

Larsen, G., Gudmundsson, M.T., and Björnsson, H. (1998). Eight centuries of periodic volcanism at the center of the Iceland hotspot revealed by glacier tephrostratigraphy. *Geology* 26:943– 946.

Major, J.J., and Newhall, C.G. (1989). Snow and ice perturbtion during historical volcanic-eruptions and the formation of lahars and floods – a global review. *Bull Volcanol* 52:1–27.

Óladóttir BA, Larsen G, Sigmarsson O (2011) Holocene volcanic activity at Grímsvötn, Bárdarbunga and Kverkfjöll subglacial centres beneath Vatnajökull, Iceland. Bull Volcanol 73(9):1187–1208.

Oddsson, B., Gudmundsson, M.T., Larsen, G., and Karlsdóttir, S. (2012). Monitoring of the plume from the basaltic phreatomagmatic 2004 Grímsvötn eruption—Application of weather radar and comparison with plume models. *Bull Volcanol* 74(6):1395–1407.

Pálsson, F., Gunnarsson, A., Jónsson, Þ., Steinþórsson, S., Pálsson, H.S., 2016. Vatnajökull: Mass Balance, Meltwater Drainage and Surface Velocity of the Glacial Year 2014–15 (Landsvirkjun report).

Pedersen GBM, Höskuldsson A, Dürig T, Thordarson T, Jónsdóttir I, Riishuus MS, Óskarsson BV, Dumont S, Magnusson E, Gudmundsson MT, Sigmundsson F, Drouin VJPB, Gallagher C, Askew R, Guðnason J, Moreland WM, Nikkola P, Reynolds HI, Schmith J (2017) Lava field evolution and emplacement dynamics of the 2014–2015 basaltic fissure eruption at Holuhraun, Iceland. J Volcanol Geotherm Res. doi:10.1016/j.jvolgeores.2017.02.027

Reynolds, H.I., Gudmundsson, M.T., Högnadóttir, Th., Magnússon, E., andPálsson, F. (2017). Subglacial volcanic activity above a lateral dyke path during the 2014–2015 Bárdarbunga-Holuhraun rifting episode, Iceland. *Bull Volcanol* 79 (6), 38.

Reynolds, H.I., Guðmundsson, M.T., Högnadóttir, Th., and Pálsson, F. (2018). Thermal power of Grímsvötn, Iceland, from 1998 to 2016: Quantifying the effects of volcanic activity and geothermal anomalies. *J Volcanol Geotherm Res*. 354: 184-193

Reynolds, H.I., Gudmundsson, M.T., Högnadóttir, Þ., and Axelsson, G. (2019). Changes in geothermal activity at Bárdarbunga, Iceland, following the 2014–15 caldera collapse, investigated using geothermal system modelling. *J Geotherm Res: SR*. doi.org/10.1029/2018JB017290

Sigmundsson F, Hooper A, Hreinsdottir S, Vogfjord KS, Ofeigsson BG, Heimisson ER, Dumont S, Parks M, Spaans K, Gudmundsson GB, Drouin V, Arnadottir T, Jonsdottir K, Gudmundsson MT, Hognadottir Th, Fridriksdottir HM, Hensch M, Einarsson P, Magnusson E, Samsonov S, Brandsdottir B, White RS, Agustsdottir Th, Greenfield T, Green RG, Hjartardottir AR, Pedersen R, Bennett RA, Geirsson H, La Femina PC, Bjornsson H, Palsson F, Sturkell E, Bean CJ, Mollhoff M, Braiden AK, Eibl EPS (2015) Segmented lateral dyke growth in a rifting event at Bardarbunga volcanic system, Iceland. Nature 517(7533):191–195.

Sigvaldason, G. (1965). The Grímsvötn thermal area. *Jökull*, 15, 125-128.

Sphera, F.J. (2000) Physical properties of magmas. In: Sigurdsson, H. (ed.) Encyclopaedia of volcanoes, Academic Press, 171-190.

Thordarson, T., and Larsen, G. (2007). Volcanism in Iceland in historical time: Volcano types, eruption styles and eruptive history. *Journal of Geodynamics* 43(1):118–152.

Zimbelman, D.R., Rye, R.O., and Landis, G.P. (2000). Fumaroles in ice caves on the summit of Mount Rainier—preliminary stable isotope, gas, and geochemical studies. *J Volcanol Geotherm Res* 97:457–473, doi: 10.1016/S0377-0273(99)00180-8.